Phases of active matter in two dimensions

Leticia F. Cugliandolo

Sorbonne Universite,
Laboratoire de Physique Theorique et Hautes Energies, CNRS UMR 7589
Tour 13, 5eme etage, 4 Place Jussieu,
75252 Paris Cedex 05, France

Giuseppe Gonnella

Universita degli Studi di Bari and INFN Sezione di Bari,
Dipartimento di Fisica,
via Amendola 173,
I-70126 Bari, Italia

OXFORD
UNIVERSITY PRESS

Preface

These notes focus on the description of the phases of matter in two dimensions. Firstly, we present a brief discussion of the phase diagrams of bidimensional interacting passive systems, and their numerical and experimental measurements. The presentation will be short and schematic. We will complement these notes with a rather complete bibliography that should guide the students in their study of the development of this very rich subject over the last century. Secondly, we summarise very recent results on the phase diagrams of active Brownian disks and active dumbbell systems in two dimensions. The idea is to identify all the phases and to relate, when this is possible, the ones found in the passive limit with the ones observed at large values of the activity, at high and low densities, and for both types of constituents. Proposals for the mechanisms leading to these phases will be discussed. The physics of bidimensional active systems open many questions, some of which will be listed by the end of the Chapter.

Acknowledgements

We want to warmly thank our collaborators on studies of active matter; in alphabetical order Mathias Casiulis, Olivier Dauchot, Pasquale Digregorio, Gianluca Laghezza, Antonio Lamura, Demian Levis, Davide Loi, Davide Marenduzzo, Alessandro Mossa, Stefano Mossa, Ignacio Pagonabarraga, Isabella Petrelli, Antonio Suma, and Marco Tarzia, from whom we learnt most of what we present in these notes. Leticia F. Cugliandolo is a member of Institut Universitaire de France. She thanks the KITP University of Santa Barbara at California (National Science Foundation under Grant No. NSF PHY17-48958) where these lectures notes were prepared in part. Our numerical work was possible thanks to allocated time at the MareNostrum Supercomputer at the Barcelona Supercomputing Center (BSC), the IBM Nextscale GALILEO at CINECA (Project INF16- fieldturb) under CINECA-INFN agreement and Bari ReCaS e-Infrastructure funded by MIUR through PON Research and Competitiveness 2007-2013 Call 254 Action I.

Contents

1
Phases of planar active matter

1.1 Introduction

These notes describe the content of a two-lecture course given by L. F. Cugliandolo at the summer school "Active Matter and Non Equilibrium Statistical Physics" held at the Les Houches School of Physics (August-September 2018). They will be published in a volume of the Les Houches collection dedicated to this school. A detailed introduction to active matter will appear in other Chapters of this book and we will not cover it here.

Our plan is to explain some of the peculiarities of passive and active matter in two dimensions. While under most natural conditions matter fills three dimensional volumes, systems can be restrained to occupy one or two dimensional spaces with convenient confining potentials. Low dimensional systems are interesting for practical and conceptual reasons. First of all, they are realised in Nature, and some classical and quantum examples are colloidal suspensions under confined conditions, liquid crystal, magnetic and superconducting films, and electrons trapped at liquid helium surfaces, to name just a few. Secondly, they can be easier to study numerically and experimentally than their higher dimensional extensions. But most importantly, they can pose specific and interesting questions of fundamental relevance. We will discuss some of these in these notes.

In the rest of the Introduction we briefly describe some salient features of equilibrium matter in $2d$ and the problems that the injection of energy poses on the analytic treatment of far from equilibrium systems. We will also state the concrete issues that we addressed in the lectures and that we will treat in the body of these notes.

1.1.1 Equilibrium: role of symmetries and space dimension

Let us start with an *aperçu* of passive matter in low dimensions. In equilibrium, the inter particle interactions are responsible for the richness and complexity of the phases in which matter can exist. Over the last century a rather good understanding of some of these phases, namely the solid, liquid and gas, and a partial understanding of more exotic cases, such as glasses or plasmas, have been reached. However, the phase diagram of matter in two dimensions is still under debate. While it is well-established that in the thermodynamic limit crystals cannot exist in two dimensions, non-crystalline solids (with a non-vanishing shear modulus[1]) do. Still, the mechanisms driving solid's melting and the transition towards the liquid phase are not fully settled yet.

[1]The shear modulus quantifies the deformation caused under a force F parallel to one of the material's surfaces while its opposite face experiences an opposing force such as friction. It is defined

Symmetries are one of the important factors that determine the collective behaviour of an equilibrium system. Two basic symmetries of the laws of nature are *translational* and *rotational* invariance. These are consequences of the fact that, typically, in systems with pairwise interactions the potential energy depends on $r_{ij} = |\mathbf{r}_i - \mathbf{r}_j|$, with $\mathbf{r}_i$ and $\mathbf{r}_j$ the positions of the two constituents, and not on $\mathbf{r}_i$ and $\mathbf{r}_j$ independently. While the state of a macroscopic system in equilibrium is expected to respect both at sufficiently high temperature and low density, in the opposite cold and/or dense limit one or both of these symmetries can be broken, and macroscopic observations may, for instance, depend on the orientation of the sample. Such a phase transition then reflects the failure of the system to respect the symmetry of its Hamiltonian.

In a crystalline phase, the constituents order in a perfect periodic and stable array that covers the sample (ignoring the typically small displacements induced by thermal fluctuations). This kind of order is said to be "long-ranged". Continuous translational invariance is broken since the lattice is invariant under translations by discrete vectors only. Moreover, the orientation of the local crystallographic axes, associated to each particle *via* its first neighbours, is always the same, and continuous rotational invariance is also broken. In a gas or a liquid both translational and rotational symmetries are respected, the constituents are randomly placed in the samples, and these are completely isotropic. In between these two extremes, there are situations in which the systems can be partially ordered, for example, exhibiting long-range orientational order but only short-range positional one, meaning that the regular arrangement of the constituents extends over a microscopic distance only, typically, a few inter constituent spacings. We shall further explore these cases here.

In low dimensional systems with short-range interactions long-range translational order is forbidden by the so-called Mermin-Wagner theorem but a solid phase with quasi long-range translational order is allowed. Roughly speaking, quasi long-range order means that although the ordered pattern is destroyed at long distances, this occurs very smoothly and, more concretely, the corresponding correlation functions decay algebraically. A proposal for the mechanism for the transition from solid to liquid led by the dissociation of dislocation pairs[2] was proposed by Kosterlitz & Thouless (KT) in their 1972 & 1973 seminal papers. However, knowing that long-range orientational order is possible in $2d$ (Mermin, 1968), Nelson and Halperin (1979) and Young (1979) modified the KT picture and claimed that the transition actually occurs in two steps, the second one being linked to the unbinding of disclinations[3] [see the sequence of upper panels in Fig. 1.4 showing configurations with four localised defects in the solid (A), dissociated dislocation pairs in the intermediate (B) and unbound disclinations in the liquid (C)]. In this picture the intermediate phase keeps quasi long-range orientational order, allowing the system to increase its entropy over the solid at a moderate energy cost.

Phase transitions have been classified by Ehrenfest according to the behaviour

as the ratio of shear stress over shear strain, $(F/A)/(\Delta x/l)$, with A the area of the surface, Δx the displacement caused by the force and l the original length. Fluids have vanishing shear modulus.

[2] A dislocation is a line, plane, or region in which there is a discontinuity in the normal lattice structure of a crystal.

[3] A disclination is a line defect in which rotational symmetry is violated.

of the free-energy as a function of the thermodynamic variables. In this framework, first and second order phase transitions exhibit a discontinuity in the first and second derivative of the free energy, respectively, while infinite order phase transitions have an essential singularity at a critical value of the control parameter (more details are given in Sec. 1.3). In the so-called KTHNY scenario, the solid-hexatic and hexatic-liquid transitions are of infinite order, *à la* KT. Part of the latter picture has been recently contested in passive systems with hard potentials (Bernard & Krauth, 2011) and we will review the modifications proposed in the body of the notes.

1.1.2 Out of equilibrium: lack of generic guiding principles

In active systems, the injection of energy adds complexity and richness to the variety of behaviours that a large system can have. In particular, one could revisit the no-go theorems for crystalline order in two dimensions, one could wonder whether the solid phases still exist and whether they are favoured or disfavoured under activity, or whether disorder phases are enhanced by the injection of energy. All these are questions that merit attention.

Much of the studies of active matter systems have focused on low density limits in which solid phases do not exist. Powerful analytical approaches, such as hydrodynamic theories, and numerical ones, such as Lattice Boltzmann methods, can be developed and successfully applied to describe the behaviour in dilute limits. These are treated in detail in other Chapters of this book. In contrast, less has been done for dense systems, cases in which even the passive limit is harder to unveil.

Another difficulty, or richness, of out of equilibrium systems is that *thermodynamic concepts* have to be revisited as they are not necessarily defined. *Effective temperatures* and chemical potentials, intensive parameters in a thermodynamic approach, have been successfully used in the context of glassy physics, see *e.g.* the review article (Cugliandolo, 2011), but become dynamic concepts that need to be measured carefully, separating time-scales and taking into account possible strong spatial heterogeneities. The definition of pressure, that appears linked to density and temperature in the equilibrium equations of state and allows one to estimate phase diagrams, also needs to be revisited out of equilibrium. Indeed, as it has been noticed in several occasions, the mechanical and thermodynamic definitions that are equivalent in equilibrium are not necessarily so out of equilibrium and the mere existence of an equation of state becomes an issue in itself.

Confronted with the difficulty of deriving analytic results for interacting many-body systems, *numerical methods* can come to our rescue and help us understanding at least some aspects of the collective behaviour of matter, especially under dense conditions and the effects of activity. In the numerical studies of the equilibrium properties of passive systems one has the freedom to choose between *molecular dynamics simulations*, in which Newton's equations of motion are integrated over sufficiently long time scales or *Monte Carlo simulations* in which non-physical transition probabilities are sometimes chosen to optimise the sampling of the equilibrium measure. In the context of active matter, the numerical integration of the actual dynamical equations is preferred [see, however, Levis and Berthier (2014) and Klamser *et al.* (2018)

for kinetic Monte Carlo methods for active systems] putting a computational limit to the size and time scales that can be studied.

1.1.3 These lectures

Concretely, the aim of these two lectures has been: (1) to expose the students to a classical problem in statistical physics, the one of order and disorder in two dimensional passive systems (possible glassy aspects have been intentionally left aside); (2) to introduce them to some standard tools used in the study of molecular systems; (3) to discuss some aspects of dense, dry, interacting active matter confined to a plane. The latter system combines the difficulties of low-dimensional passive matter and the effects introduced by the constant injection of energy that is partially dissipated and partially used by the system itself. It is a challenging kind of problem with many open routes for further study, some of which are discussed by the end of the notes.

Concretely, the rest of the notes are structured as follows. Firstly, we introduced and discuss the definition of a couple of standard agent-based models in Sec. 1.2. Secondly, we gave a short reminder of the definitions and properties of phase transitions of second, first and infinite order in Sec. 1.3. Thirdly, we recall some features of equilibrium phases in two dimensions in Sec. 1.4. Fourthly, in Sec. 1.5 we present some recent results on the phase diagrams of the two models defined in Sec. 1.2. Finally, in Sec. 1.6 we present some conclusions and lines for future research.

1.2 Models and observables

Numerous models of active matter exist in the literature but we will not explain them all here. We will instead focus on some that are directly inspired by the microscopic modelling of atomic and molecular passive systems, and hence admit a clear and simple equilibrium limit. Such agent based active matter models make choices on (1) the form of the constituents, (2) the inter-particle interactions, (3) the coupling to the solvent or medium in which the agents are immersed, (4) the way in which the activity acts, and (5) the dimension and form of the confining space. In Sec. 1.2.1 we list and discuss some common choices made on these five properties. Besides, in Sec. 1.2.2 we define and discuss some observables that serve to characterise order (or the lack of it) in molecular systems, and that we will use to find the phases of the active problem.

1.2.1 Models

The form of the constituents. Playing with individual spheres one can switch from "atomic" to "molecular" models. More precisely, the constituents can be chosen to be simply spherically symmetric objects (*disks* in two dimensions), two of them can be linked together with a spring or a rod to form a *dumbbell*, or one can join many of them to build a *polymer*. As well-known in the studies of passive liquids in equilibrium and out of equilibrium, the behaviour of an ensemble of such various objects can be rather different. Important shape effects have also been found in active matter and we will discuss some of them here.

Specifically, a disk is a spherically symmetric planar object with mass m_{d} and diameter σ_{d}. A dumbbell is a diatomic molecule made of two such disks linked together with a massless spring or a rigid rod. There is a polarity associated to the dumbbells,

with the each disk playing a head or tail role. Adding more such monomers one can also build polymers of any desired length with adequate bending properties.

Coupling to the environment. The dissipation and fluctuations induced by the coupling to the environment are commonly mimicked *à la* Langevin, by adding friction and noise terms to the equations of motion. After inspection of the different time-scales involved in the motion of the active (Brownian) particles and the constituents of the environment, in standard experimental settings a Markovian (no memory) assumption is justified (similarly to what is often done for passive Brownian particles). The noises are then chosen to be Gaussian, with zero mean and delta correlations proportional to the friction coefficient $\gamma_{\rm d}$ and the temperature of the bath T: $\langle \xi_i^a(t)\, \xi_j^b(t')\rangle = 2\gamma_{\rm d} k_B T \delta_{ij} \delta(t-t')\delta_{ab}$, with $a, b = 1, \ldots, d$ and d the dimension of space, and i, j particle indices. The Boltzmann constant is denoted k_B.

The active Brownian disks equations of motion. The dynamics of active Brownian disks is usually studied in the over-damped limit. The particles self-propel under a constant modulus force $F_{\rm act}$ along a (rotating) direction $\mathbf{n}_i = (\cos\theta_i(t), \sin\theta_i(t))$ attached to the particle with θ_i the angle formed with a fixed axis. The disk center positions obey

$$\gamma_{\rm d}\dot{\mathbf{r}}_i = -\boldsymbol{\nabla}_i \sum_{j(\neq i)} U(r_{ij}) + F_{\rm act}\mathbf{n}_i + \boldsymbol{\xi}_i \ , \qquad \dot{\theta}_i = \eta_i \ . \tag{1.1}$$

In the first equation $\gamma_{\rm d}$ is the friction coefficient, U is the inter-particle potential, $\boldsymbol{\nabla}_i = \partial_{\mathbf{r}_i}$, $F_{\rm act}$ is the strength of the active force, and $\boldsymbol{\xi}_i$ is a vectorial white noise as the one described in the previous paragraph. $i, j = 1, \ldots, N$ are labels that run over all particles in the system. The angular noise is taken to be Gaussian with zero mean and correlations $\langle \eta_i(t)\eta_j(t')\rangle = 2D_\theta \delta_{ij}\delta(t-t')$. The units of length, time and energy are given by σ_d, $\tau = D_\theta^{-1}$ and ε, respectively. The angular diffusion coefficient is commonly fixed to $D_\theta = 3k_BT/(\gamma_{\rm d}\sigma_d^2)$ (apart from the unimportant numerical factor that depends on the form of the objects, this is also the angular diffusion coefficient of a single active dumbbell).

The active dumbbells equations of motion. We model the time evolution of each sphere in the dumbbell through a Langevin equation of motion that acts on the position of the centre of each bead, $\mathbf{r}_i$, and is given by

$$m_{\rm d}\ddot{\mathbf{r}}_i = -\gamma_{\rm d}\dot{\mathbf{r}}_i - \boldsymbol{\nabla}_i \sum_{j(\neq i)} U(r_{ij}) + \mathbf{F}_{{\rm act}\, i} + \boldsymbol{\xi}_i \ , \tag{1.2}$$

where $i = 1, \ldots, 2N$ is the sphere index and, again, $\boldsymbol{\nabla}_i = \partial_{\mathbf{r}_i}$. Since the noises acting on the two beads that form a dumbbell are independent, the combined stochastic force can make the dumbbells rotate.

In cases in which the inertial time-scale $m_{\rm d}/\gamma_{\rm d}$ is much shorter than all other interesting time-scales in the problem, one can take an over-damped limit and basically drop the term $m_{\rm d}\ddot{\mathbf{r}}_i$ from the equations of motion. (These cases are common in the Langevin description of the random motion of particles and molecules.) In this limit,

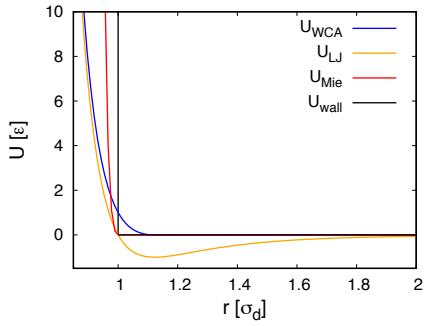

Fig. 1.1 A sketch of the Lennard-Jones ($n = 6$) potential, the WCA truncated and translated $n = 6$ one, a hard wall and a truncated and shifted Mie ($n = 32$) potential, see the text for their definitions.

the equations of motion are first order in the time derivative, as in Eqn. (1.1), but the form of the molecules and in particular the (averaged) length between the colloidal centres will have a notable importance in the collective behaviour of the macroscopic system.

Inter-particle interactions. In atomic systems the potential typically has an attractive tail due to Van der Waals dipole-dipole interactions that decays as a power law $-1/r^6$ at large separations r while at short distances the overlap of the electron clouds makes the potential strongly repulsive. The minimum of the potential, located at a distance of a few Angstroms with a value of a hundred Kelvin, is responsible for the formation of crystals. This kind of potential is also used to describe the interactions between colloidal particles in a solvent although the length and energy scales involved can be very different from the atomic ones (say, length scales between a nanometer and a micrometer). In some cases, only the repulsive part that accounts for the excluded volume interaction between colloids is retained. Without entering into a detailed justification for the latter choice, it is commonly adopted in the context of active matter as well. The potential is then taken to be a generalised Lennard-Jones (LJ) of Mie type (Mie, 1903), truncated and shifted à la Week-Chandler-Andersen (WCA, 1971): calling $\mathbf{r}_i$ the d-dimensional position of the centre of the ith particle and $r = |\mathbf{r}_i - \mathbf{r}_j|$ the inter-particle distance, the short-ranged repulsive potential takes the form

$$U(r) = \begin{cases} 4\varepsilon\left[(\sigma/r)^{2n} - (\sigma/r)^{n}\right] + \varepsilon & \text{if} \quad r < \sigma_{\mathrm{d}} = 2^{1/n}\sigma\,, \\ 0 & \text{otherwise}\,, \end{cases} \tag{1.3}$$

with n a parameter that tunes the softness of the potential ($n = 6$ is the usual LJ one and increasing n the potential gets harder), ϵ an energy scale and σ a length scale chosen to be of the order of the particle diameter. The hard wall, LJ, WCA, and the very steep Mie with $= 32$ potentials are compared in Fig. 1.1.

Activity. The active forces can be persistent or not. Persistency means that the constituents have a preferred direction along which the active force is permanently applied.

For instance, in the dumbbell models, the molecules are elongated along a main axis, with each bead having a head or tail nature. The active force is always exerted along this axis from tail to head (Cugliandolo et al., 2017; Petrelli et al., 2018). An example with non-persistent activity is the one treated in Loi *et al.* (2011), a polymeric model in which the active force was applied on temporal intervals of a given duration only, on a preselected monomer, and with random direction. In the case of the active Brownian disks, these are assumed to have a direction attached to them, along which the active force is always applied (Henkes, Fily and Marchetti, 2011; Fily and Marchetti, 2012; Redner, Hagan and Baskaran, 2013; Fily, Henkes and Marchetti, 2014; Redner, Wagner, Baskaran and Hagan, 2016).

The Péclet number. The Péclet number is a dimensionless parameter defined as $\mathrm{Pe} = F_{\mathrm{act}}\sigma_{\mathrm{d}}/(k_BT)$ that quantifies the strength of the activity as compared to the thermal fluctuations. It has a twofold interpretation. One is as a ratio between the advective transport, say $\ell v = F_{\mathrm{act}}\sigma_{\mathrm{d}}/\gamma_{\mathrm{d}}$ and the diffusive transport $D = k_BT/\gamma_{\mathrm{d}}$. The other one is as the ratio between the work done by the active force when translating the disk by its typical dimension, $F_{\mathrm{act}}\sigma_{\mathrm{d}}$, and the thermal energy, k_BT. The Péclet number can be tuned by changing F_{act} at fixed γ_{d} and k_BT, for example.

Reynolds number. The Reynolds number confronts the strength of the inertial force to the viscous one $\mathrm{Re} = \rho L v/\mu = (\sigma_{\mathrm{d}}F_{\mathrm{act}}/\gamma_{\mathrm{d}})/(\gamma_{\mathrm{d}}\sigma_{\mathrm{d}}^2/m) = m_{\mathrm{d}}F_{\mathrm{act}}/(\gamma_{\mathrm{d}}^2\sigma_{\mathrm{d}})$ and it is typically very small, say 10^{-2}, for the values of the parameters used in the simulations.

Space and packing fraction. The constituents are typically confined to displace themselves in a d dimensional box with linear length L and periodic boundary conditions, a situation that minimises finite size effects and evades the difficulty of modelling the interactions with the boundary walls. The packing fraction is then defined as $\phi = \pi\sigma_d^2 N/(4L^d)$ (with an extra factor of 2 for the dumbbells, for which the distance between the centres of the two coloids is fixed to σ_{d}) and can be tuned by changing N or L, for example.

1.2.2 Observables

In this Section we define a number of observables and correlation functions that are used to characterise positional and orientational order in molecular systems. In all the definitions we keep the time-dependence to evaluate the possible evolution of these quantities and thus quantify the dynamics of the problem.

Voronoi tessellation. The first issue we want to resolve is to attribute a notion of neighbourhood to particles in the configurations. This is done with the help of a Voronoi tessellation. In our problem, we start by assigning N points on the plane to the centres of the disks, be them the individual particles or the beads building the diatomic molecules. We then partition space in areas such that each space point is closer to the centre of one disk than to any other one. Each particle is therefore uniquely enclosed by each such polygon. The borders of the areas thus constructed are polygons and the number of neighbours of a point is given by the number of sides of the polygon, see the sketch in Fig. 1.2 (a). An example of a concrete dumbbell configuration with its Voronoi tessellation is shown in Fig. 1.3 (a).

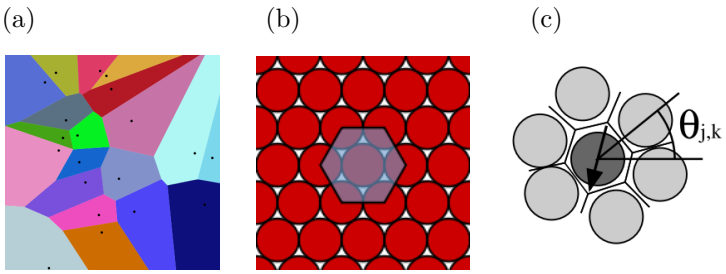

Fig. 1.2 (a) An example of Voronoi tessellation. (b) Close packing of disks, the hexagonal lattice. (c) The definition of the angle θ_{jk} between a bond and a reference (horizontal) axis. The local hexatic order parameter represented as a vector attached to the central particle. The two last panels have been borrowed from E. Bernard's PhD thesis.

Fluctuating local density. One can measure *local densities* ϕ_j, with a discrete index dependence, in at least two ways, and construct with them histograms and probability distribution functions.

With the first method, for each bead, one first estimates the local density as the ratio between its surface and the area of its Voronoi region $A_j^{\rm Vor}$. This value can then be coarse-grained by averaging the single-bead densities over a disk with radius R around the concerned bead,

$$\phi_j(t) = \frac{1}{n_R^{(j)}(t)} \sum_{i \in S_R^{(j)}} \frac{\pi \sigma_{\rm d}^2}{4 A_i^{\rm Vor}(t)} \ . \tag{1.4}$$

where $n_R^{(j)}$ and $S_R^{(j)}$ are the number of particles and the set of particles placed inside the spherical disk with radius R around the jth bead, respectively.

With the second method, one constructs a square grid on the simulation box, for each point in the grid one calculates a coarse grained local density ϕ_j over a circle of given radius R, and one finally assigns this density value to the grid point.

A visual inspection of the density fluctuations in real space is achieved by painting with the colour that corresponds to its coarse-grained local density each Voronoi region. Typically, a heat map with the convention denser in yellow and looser in violet, is used. The dumbbell configuration in Fig. 1.3 (a) is analysed along these lines and the local densities are painted according to such a colour code in panel (b).

Positional order. The fluctuating local density field is defined as

$$\rho(\mathbf{r}, t) = N^{-1} \sum_{i=1}^{N} \delta(\mathbf{r} - \mathbf{r}_i(t)) \ , \tag{1.5}$$

where the sum runs over particle indices, $\mathbf{r}_i(t)$ is the time-dependent position of the ith particle, and N is the total number of particles. The quantity is normalised to one $\int d^d\mathbf{r}\, \rho(\mathbf{r}, t) = 1$. In a homogeneous system $\rho(\mathbf{r}, t) = \rho_0 = 1/V$ with $V \equiv \int d^d\mathbf{r}$ the volume of the box where the system is confined.

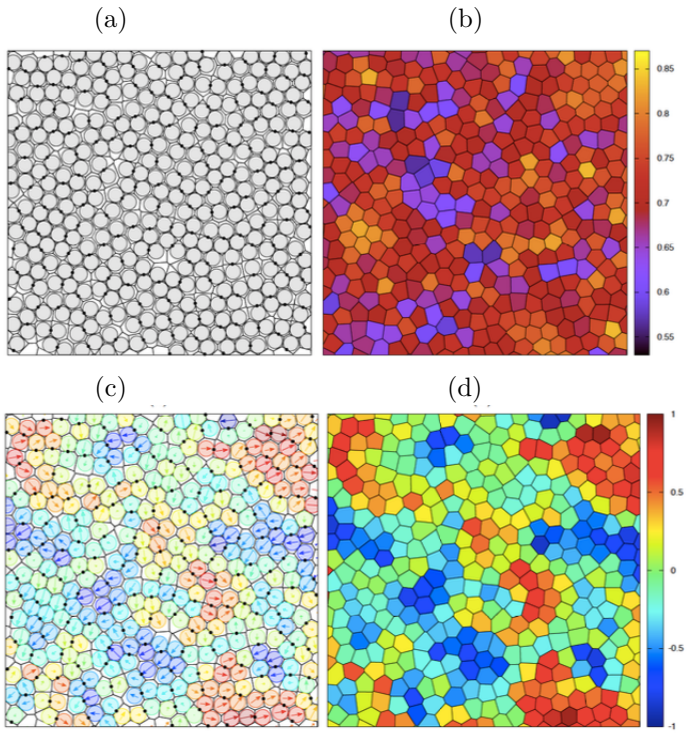

Fig. 1.3 (a) The Voronoi tessellation of a dumbbell configuration (the joining point between the two beads is shown with a dark spot). (b) The heat map attributed to the local density of the individual disks, with their own Voronoi cells painted accordingly. In panels (c) and (d) the cells are painted following the heat map attributed to the projection of the local hexatic order parameter in the direction of its mean value. In (c) the arrows are still drawn and light colours are used while in (d) the arrows have been erased and darker colours are chosen.

The density-density spatial correlation function

$$C(\mathbf{r}_1, \mathbf{r}_2, t) = \langle \rho(\mathbf{r}_1, t)\rho(\mathbf{r}_2, t)\rangle \tag{1.6}$$

involves an average over different realisations of the system henceforth represented by the symbol $\langle \ldots \rangle$. This quantity is, for a homogeneous system, space translational invariant meaning that it only depends on $\mathbf{r}_1 - \mathbf{r}_2 = \mathbf{r}$. If, moreover, the density is isotropic, $C(\mathbf{r}_1, \mathbf{r}_2, t) = C(|\mathbf{r}_1 - \mathbf{r}_2|, t)$.

The Fourier transform of the density-density correlation yields the *structure factor*

$$S(\mathbf{q}, t) = \int d^d\mathbf{r}_1 \int d^d\mathbf{r}_2 \; NC(\mathbf{r}_1, \mathbf{r}_2, t)\; e^{-\mathrm{i}\mathbf{q}\cdot(\mathbf{r}_1 - \mathbf{r}_2)} = \frac{1}{N}\sum_{ij}\langle e^{-\mathrm{i}\mathbf{q}\cdot(\mathbf{r}_i(t) - \mathbf{r}_j(t))}\rangle \; . \tag{1.7}$$

A real order parameter related to possible translational order is the modulus of the Fourier transform of the density

$$\psi_T(\mathbf{q},t) = \left| N^{-1} \sum_{i=1}^{N} e^{\mathrm{i}\mathbf{q}\cdot\mathbf{r}_i(t)} \right|^2 . \tag{1.8}$$

The positional order can be tested with correlations of the Fourier transform of the density

$$C_{\mathbf{q_0}}(r,t) = \langle e^{\mathrm{i}\mathbf{q_0}\cdot(\mathbf{r}_i(t)-\mathbf{r}_j(t))} \rangle \tag{1.9}$$

where $r = |\mathbf{r}_i(t) - \mathbf{r}_j(t)|$ and $\mathbf{q}$ is taken to be $\mathbf{q_0}$ the wave vector that corresponds to the maximum value of the first diffraction peak of the structure factor (1.7). The quasi-long range positional order in the solid phase should be evidenced by an algebraic decay of $C_{\mathbf{q_0}}(r)$ with distance. Instead, in the hexatic and liquid phases the decay of $C_{\mathbf{q_0}}(r)$ should be exponential, see Fig. 1.4.

Orientational order. The order parameter for orientational order is the local time-dependent n-fold order parameter

$$\psi_{n\,i}(t) = \frac{1}{N^i_{\mathrm{nn}}} \sum_{k(i)}^{N^i_{\mathrm{nn}}} e^{\mathrm{i}n\theta_{ki}(t)} , \tag{1.10}$$

where $\theta_{ki}(t)$ is the instantaneous angle formed by the bond that links the ith bead with the kth one, the latter being a first neighbour on the Voronoi tessellation of space, and a chosen reference axis, see Fig. 1.2 (c). The sum runs over the N^i_{nn} first neighbours of the disk i and n is an integer to be chosen according the expected orientational order, $n = 6$ in our cases.

The ground state of a system of spherically symmetry constituents interacting *via* Lennard-Jones-like potentials is expected to be a perfect hexagonal lattice; for a recent review on the search for ground state configurations, written from a mathematical perspective, see Blanc & Lewin (2015). For beads regularly placed on the vertices of such a lattice, see Fig. 1.2 (b), each site has six nearest-neighbours and all the angles are, $\theta_{ki} = 2\pi k/6 + \phi$ where ϕ is just an arbitrary phase coming from the misalignment between the bonds and the lab axis. The relevant value of n to use is 6, for which $\psi_{6i} = 1$ on a perfect hexagonal lattice. At finite temperature this parameter becomes less than one.

A colour code is useful to detect local orientational order. The plane is first divided in cells according to the Voronoi prescription, see Figs. 1.2 (a) and 1.3 (a). Next, an arrow representing the local (complex) order parameter is attributed to each cell, see Fig. 1.3 (c). The average over all cells is computed yielding a vector of given modulus and direction. The local arrows are then projected on the direction of the averaged vector. The cells with maximal projection are coloured in red, the cells with maximal projection in the opposite direction are coloured in blue, and the scale in between is colour coded as in the right bar in Fig. 1.3 (d).

Upon coarse-graining over a cell with radius R around a point $\mathbf{r}$ that possibly contains a large number of particles, say n_R, one can build histograms and then probability distribution functions of the coarse-grained local hexatic order parameter

$$\psi_n^{\rm cg}(\mathbf{r},t) = \frac{1}{n_R}\sum_{i\in S_R^{(\mathbf{r})}} \frac{1}{N_{\rm nn}^i}\sum_{k(i)} e^{{\rm i}n\theta_{ki}(t)} \ . \tag{1.11}$$

$S_R^{(\mathbf{r})}$ is the set of particles inside the disk with radius R centered at the point $\mathbf{r}$. With the complex order parameter (1.10), or with its coarse-grained version, one then constructs a real correlation function

$$C_n(r,t) = \frac{\langle \psi_{ni}^*(t)\psi_{nj}(t)\rangle_{r=|\mathbf{r}_i-\mathbf{r}_j|}}{\langle \psi_{ni}^*(t)\psi_{ni}(t)\rangle} \tag{1.12}$$

where homogeneity and isotropy have been assumed on the left-hand-side, with the simple dependence on $r = |\mathbf{r}_i - \mathbf{r}_j|$.

The hexatic order parameter and its correlations probe the bond-orientational order thus allowing the liquid, hexatic and solid phases to be distinguished: the decay should be exponential in the liquid, power law in the hexatic and approach a constant in the solid, see Fig. 1.4.

Defects. From the Voronoi tessellation of space one can count the number of neighbours that any particle has. Deviations from the value 6, the one that a perfect hexagonal lattice would have, as in Fig. 1.2 (b), are defects, typically corresponding to particles having 5 or 7 neighbours. The sketches in Fig. 1.4 show the behaviour of the defects, according to the KTHNY scenario: the defects are bound to each other in pairs and can freely move without destroying the quasi long-range translational and long-range orientational order in the solid (A), they unbind in pairs in the hexatic (B) and they get free in the liquid (C). In actual fact, recent simulations (Qi, Gantapara and Dijkstra, 2014) show that defects get together in clusters, which tend to be small and compact in the hexatic phase, but become string-like (grain boundaries) in the region with coexistence of hexatically ordered and liquid and also in the liquid phase. This is one of the issues that deserves a better analysis in the future, both for passive and active systems.

Time delayed correlation functions. The use of time correlation functions in experiments, instead of spatial ones, has the advantage that due to the limited field of view, the latter cannot be obtained over a large dynamic range, while the former can, in principle, cover arbitrarily many decades. Time-delayed correlation functions simply compare the value of an observable at a time t_1 with the value of the same observable at a later time t_2. The result is a function of $t_2 - t_1$ under stationary conditions. The exponential or algebraic decays of spatial correlations as a function of distance in the various phases is translated into exponential or algebraic decays as functions of the time-delay $t_2 - t_1$ in the temporal correlations.

Mean-square positional displacement. The simplest time-delayed observable that characterises the translational properties of the elements in the samples is probably the averaged mean-square displacement of the position of a relevant point on the molecules, be it the centre of the disks or the centre of mass,

$$\Delta_r(t_2 - t_1) = \frac{1}{dN}\sum_i \langle |\mathbf{r}_i(t_2) - \mathbf{r}_i(t_1)|^2\rangle \tag{1.13}$$

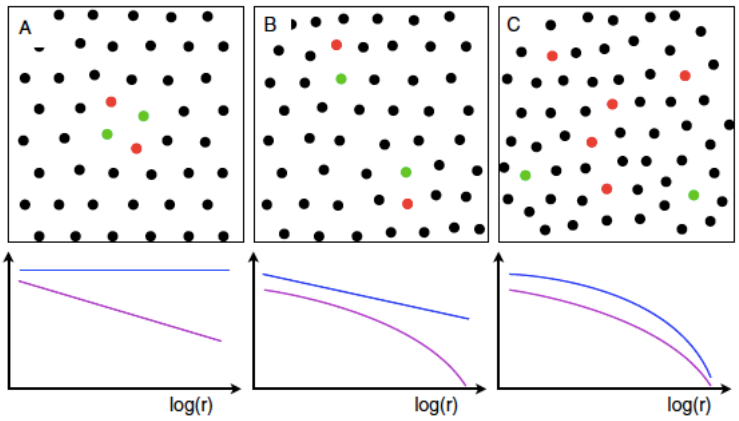

Fig. 1.4 Sketch of configurations with defects of various kinds (top panels) and the correlation functions (bottom panels) in the solid, hexatic and liquid phases. Image taken from Gasser (2009). Red (green) points are particles with five (seven) neighbours. The sketch in A is in the solid phase, the one in B in the hexatic phase and the one in C in the liquid phase. In the three lower panels, the (blue) curves lying above are the correlations $C_6(r)$ that quantify the orientational order while the (purple) curves lying below are the correlations $C_{\mathbf{q}_0}(r)$ that measure translational order.

with the angular brackets denoting average over the noises and the times being such that $t_2 \geq t_1$.

Angular mean-square displacement. Another characterisation of the global dynamics, that focuses on the rotational properties of the constituents, is given by the averaged mean-square displacement of the angles formed by a relevant direction of the molecule and a chosen axis of reference,

$$\Delta_\vartheta(t_2 - t_1) = \frac{1}{N}\sum_i \langle |\vartheta_i(t_2) - \vartheta_i(t_1)|^2 \rangle \ . \tag{1.14}$$

The Lindemann criterium. The dynamic Lindemann parameter (Zahn, Lenke and Maret, 1999) is

$$\gamma_L(t) = \langle |[\mathbf{r}_i(t) - \mathbf{r}_i(0)] - [\mathbf{r}_j(t) - \mathbf{r}_j(0)]|^2 \rangle / (2a^2) \tag{1.15}$$

with i and j first neighbour particles at the initial time $t = 0$, say, and a the crystalline lattice spacing. In a crystal $\gamma_L(t)$ is bounded at long times while in the liquid the displacements of the two particles are uncorrelated and $\gamma_L(t) = \langle |\mathbf{r}_i(t) - \mathbf{r}_i(0)|^2 \rangle / (2a^2) + \langle |\mathbf{r}_j(t) - \mathbf{r}_j(0)|^2 \rangle / (2a^2)$ is just the mean-square displacement of an individual particle, see Eqn. (1.13), and it is then proportional to t (simple diffusion). The change from bounded behaviour to time-increasing one can be used as evidence for the end of the solid phase.

1.3 A reminder on phase transitions

This Section contains a (very) rapid reminder of phase transitions with emphasis on properties and concepts that are useful for our purposes. Many textbooks give detailed descriptions of critical phenomena (Stanley, 1971; Amit, 1984; Parisi, 1988; Goldenfeld, 1992; Cardy, 1996; Simon, 1997; Herbut, 2006; Kardar, 2007).

1.3.1 First order

In a first-order phase transition a state that is stable on one side of the transition, becomes metastable on the other side of it. The order parameter jumps at the transition, for example, from zero in the disordered phase to a non-vanishing value in the ordered one. The correlation length, that is extracted from the correlations of the fluctuations of the order parameter with respect to its average, is always finite.

In common discussions of this kind of transition, the interplay between only two states is considered, each one being the preferred one on the two sides of the transition. But this is not necessarily the case and a competition between various equivalent stable states can also arise. The dynamics of first order phase transitions is driven by nucleation of the new stable phase within the metastable one in which the system is placed initially. During a long period of time the system attempts to nucleate one or more bubbles of the stable phase until some of them reach the critical size and then quickly grow. In the multi-nucleation problem, two possibilities then arise: either one of them rapidly conquers the full sample or many of them touch, get stuck, and a new coarsening process establishes. The latter case is the one that will be of interest in the hexatic-liquid transition, as we will argue below.

1.3.2 Second order

In a second-order phase transition a state that is stable on one side of the transition, becomes unstable on the other side of it and, typically, divides continuously into an even number of different stable points, related in pairs by symmetry. The order parameter is continuous at the transition and, for example, it grows from zero in the ordered phase. The correlation length, also extracted from the correlations of the fluctuations of the order parameter with respect to its average, diverges algebraically on both sides of the transition.

When the parameters are taken across the critical value, the system needs to accommodate to the new conditions and it does progressively, by locally ordering domains of each of the possible and equivalent new equilibrium states. The latter process is called coarsening or domain growth and, although it is a very general phenomenon, its details depend on some characteristics of the problem as the conservation laws and the dimension of the order parameter. The symmetry breaking process, whereby one of the equivalent equilibrium states conquers the full sample, is achieved late after the system is taken across the phase transition. Indeed, equilibration takes a time that scales with the system size and diverges in the thermodynamic limit.

1.3.3 Infinite order

Berezinskii-Kosterlitz-Thouless (BKT) phase transitions (Berezinskii, 1971a; Berezinskii, 1971b; Kosterlitz and Thouless, 1972; Kosterlitz and Thouless, 1973; Kosterlitz,

1974; Kosterlitz, 2016) lack an order parameter taking a non-vanishing value on one side of the transition (in the thermodynamic limit) and are not related to spontaneous symmetry breaking. They are transitions of a different kind, driven by the unbinding of topological defects when a critical value of a control parameter (typically temperature over an energy scale) is reached. In the disordered phase the density of free topological defects is finite and the correlation function of the would-be order parameter decays exponentially, with a correlation length that is proportional to the distance between unbound defects. This length diverges exponentially at the transition and remains infinite in the full quasi-long-range ordered phase. Topological defects exist in the ordered phase but they bound in pairs and localised in space. The divergence of the correlation length implies that the correlations of the would-be order parameter decay algebraically beyond the transition, that the system has quasi long range order and that this full phase behaves as a critical point. In terms of the associated susceptibility, it is finite in the disordered phase and it diverges in the full subcritical phase. Even more so, the transition is characterised by essential singularities in all thermodynamic functions thus receiving the "infinite" order qualification. This behaviour is due to (spin or density) wave excitations with a linear dispersion relation at long wave-lengths.

The dynamics of such phase transitions is characterised by the growth of the quasi-long-range order and the annihilation of topological defects, see, *e.g.* Jelić & Cugliandolo (2011) for a numerical study of the $2d$XY model or Comaron *et al.* (2018) for a similar analysis of a driven-dissipative bidimensional quantum system.

1.3.4 From infinite to first order

The picture described above has been developed based on the analysis of the $2d$ XY model in which planar spins are placed on the vertices of a regular lattice, with nearest neighbour pairwise interactions $-J\mathbf{s}_i \cdot \mathbf{s}_j = -J\cos\theta_{ij}$ with θ_{ij} the angle between the two spins at the i and j sites. Interestingly enough, the nature of the transition can change dramatically if the interaction term takes other forms that still respect rotational invariance. The potential $2[1-\cos^{2p^2}(\theta_{ij}/2)]$, that interpolates between the conventional one for $p=1$ and a much steeper well for large p^2, was used by Domany, Schick and Swendsen (1984) to show that the transition crosses over from BKT to first order for large p^2, see also Jonsson, Minnhagen and Nylen (1993) and Zukovic and Kalagov (2017) for a more recent and complete analysis of the Langevin and Monte Carlo studies of the same model, respectively. In particular, for $p^2 = 50$ the transition is very sharp with a huge peak in the specific heat and many other elements of a first order phase transition. The reason for this behaviour is that the typical temperature for the unbinding of vortex-antivortex pairs is pushed to very high values, beyond the ones at which other kinds of excitations drive the discontinuous transition. Similarly, other examples of models expected to have BKT transitions, such as the $2d$ Coulomb gas, were shown to comply with these expectations only at low density and depart towards a first order phase transition at higher density (Minnhagen, 1987).

1.3.5 Two results against common wisdom

Breakdown of universality. The phenomena described by the end of the last Subsection seem to be in contradiction with the picture that emerges from the renormalisation group theory according to which systems in the same universal class (having the same symmetry of the order parameter, same dimensionality and same range of the interactions) should exhibit the same type of phase transition. More precisely, universality states that the set of critical exponents that describe the behaviour of physical quantities near a continuous phase transitions, be it of second or infinite order, should be identical. However, a rigorous proof that planar spin models of the XY kind with a sufficiently narrow potential undergo first order phase transitions was provided by van Enter & Shlosman (2002) and the fact that with a simple change of parameter one can change the order of the transition was thus confirmed.

Continuous symmetry breaking in two dimensions. It is commonly found in the literature that the content of the Mermin-Wagner theorem is that "two-dimensional systems with a continuous symmetry cannot have a spontaneous broken symmetry at finite temperature". This, however, is not true in general and it was not claimed by these authors either. The Mermin-Wagner result is that the expected order parameters vanish in a number of two dimensional cases, including superfluids, superconductors, magnets, and crystals, but it does not imply that there cannot be long-range order of another kind. The spontaneous breaking of orientational order in $2d$, that was already anticipated by Landau himself (Landau, 1937a; Landau, 1937b), is a counter example of the statement between inverted commas. Indeed, broken translational symmetry implies broken rotational symmetry. However, the converse is not true and it is possible to break rotational invariance without breaking translational invariance. The most obvious way to do it is to use anisotropic molecules, as in liquid crystal systems. Another way is by achieving long-range *bond orientational* order with spherically symmetric constituents.

1.4 Equilibrium phases in two dimensions

In this Section we recall some properties of passive matter in equilibrium. We focus on two representative cases. We take a dense system at low temperatures and we evaluate the effect of thermal fluctuations. We consider a loose system and we derive the virial expansion that leads to the equation of state. These two well-known problems have intriguing extensions when activity is added, issues that we will cover in the next Section.

1.4.1 Effects of fluctuations on dense systems: melting in low dimensions

Consider a sufficiently dense system so that it should be a solid, possibly in a crystalline phase and evaluate the effect of thermal fluctuations. Does the solid melt? Which are the mechanisms leading to melting? Which is the order of the phase transition taking the solid into a liquid?

Positional vs. orientational order. In the 30s Peierls (1934) and Landau (1937a, 1937b) argued that it is not possible to find long-range positional order in low dimensional systems with short-range interactions.

Peierls used the simplest possible model for a solid, one of beads placed on a d-dimensional lattice, with Hookean couplings between nearest-neighbours, in canonical equilibrium. The question he asked was whether such a system could sustain periodic order over long distances under thermal fluctuations, and he concluded that this is not possible in $d \leq 2$, while it is in $d \geq 3$. Landau based his arguments instead on his theory of phase transitions and reached the same conclusion. In the 60s, the numerical simulations of Alder and Wainwright (1962) pointed towards a first order phase transition between solid and liquid. A more general proof of absence of crystalline order in $2d$, that does not rely on the harmonic approximation but uses a classical limit of Bogoliubov's inequality (Bogoliubov, 1962), was given later by Mermin (1968).

An equilibrium amorphous state has a uniform averaged density $\langle\rho\rangle = \rho_0$, while a zero temperature crystalline state has a periodic one

$$\rho(\mathbf{r}) = \sum_i \delta(\mathbf{r} - \mathbf{R}_i) \tag{1.16}$$

with i a label that identifies the particles or lattice sites, and $\mathbf{R}_i$ the position of the ith vertex of the lattice. At zero temperature a perfectly ordered state, with periodic density is allowed for all $d \geq 1$. However, thermal fluctuations make the atoms vibrate around their putative lattice sites, and the instantaneous position of the ith atom becomes

$$\mathbf{r}_i = \mathbf{R}_i + \mathbf{u}_i = \mathbf{R}_i + \mathbf{u}(\mathbf{R}_i) \tag{1.17}$$

with $\mathbf{u}_i = \mathbf{u}(\mathbf{R}_i)$ its displacement from $\mathbf{R}_i$. A simple way to see the lack of positional order in low dimensions (and the existence of it in higher dimensions) is to compute the mean-square displacement of the atoms assuming thermal equilibrium. Take a generic pair-wise potential

$$U_{\rm tot} = \frac{1}{2}\sum_{ij} U(\mathbf{r}_i - \mathbf{r}_j) = \frac{1}{2}\sum_{ij} U(\mathbf{R}_i - \mathbf{R}_j + \mathbf{u}_i - \mathbf{u}_j)\,. \tag{1.18}$$

Indeed, the total harmonic potential energy is (Ashcroft and Mermin, 1976)

$$\begin{aligned} U_{\rm tot} &= U_{\rm gs} + \frac{1}{2}\sum_{ij}\sum_{\mu\nu}(u_i^\mu - u_j^\mu)\,\frac{\partial^2 U}{\partial_{r_i^\mu}\partial_{r_j^\nu}}(\mathbf{R}_i - \mathbf{R}_j)\,(u_i^\nu - u_j^\nu) \\ &= U_{\rm gs} + \frac{1}{2}\sum_{ij}\sum_{\mu\nu} u_i^\mu D_{\mu\nu}(\mathbf{R}_i - \mathbf{R}_j) u_j^\nu \end{aligned} \tag{1.19}$$

where $U_{\rm gs} = \frac{1}{2}\sum_{i\neq j} U(\mathbf{R}_i - \mathbf{R}_j)$, and in the second term μ, ν run from 1 to d, $D_{ij}^{\mu\nu} \equiv D_{\mu\nu}(\mathbf{R}_i - \mathbf{R}_j) = \delta_{ij}\sum_k \phi_{ik}^{\mu\nu} - \phi_{ij}^{\mu\nu}$ and $\phi_{ik}^{\mu\nu} = \partial^2 U(\mathbf{r})/\partial r_i^\mu \partial r_k^\nu$. Three symmetries of the couplings follow immediately $D_{ij}^{\mu\nu} = D_{ji}^{\nu\mu}$, $D_{ij}^{\mu\nu} = D_{ji}^{\mu\nu}$ (from the inversion symmetry

of a Bravais lattice), and $\sum_i D_{ij}^{\mu\nu} = 0$ (from the uniform translation invariance of the full lattice). After a Fourier transform $U_{\rm tot}$ becomes

$$U_{\rm tot} = U_{\rm gs} + \frac{1}{2}\sum_{\mathbf{k}}\sum_{\mu\nu} \tilde{u}_\mu^*(\mathbf{k})\tilde{D}_{\mu\nu}(\mathbf{k})\tilde{u}_\nu(\mathbf{k}) \;, \tag{1.20}$$

where $\tilde{u}_\mu(\mathbf{k}) = \sum_i e^{i\mathbf{k}\cdot\mathbf{r}_i}\mathbf{u}_i$ and $\tilde{u}_\mu^*(\mathbf{k}) = \tilde{u}_\mu(-\mathbf{k})$ since $\mathbf{u}_i$ is real. Next one needs to estimate the $\mathbf{k}$ dependence of $\tilde{D}_{\mu\nu}(\mathbf{k})$. Using the symmetries of $D_{ij}^{\mu\nu}$, its Fourier transform $\tilde{D}_{\mu\nu}(\mathbf{k})$ can be recast as

$$\tilde{D}_{\mu\nu}(\mathbf{k}) = -2\sum_{\mathbf{R}} D_{\mu\nu}(\mathbf{R})\sin^2(\mathbf{k}\cdot\mathbf{R}/2) \approx -2\sum_{\mathbf{R}} D_{\mu\nu}(\mathbf{R})(\mathbf{k}\cdot\mathbf{R}/2)^2 \;, \tag{1.21}$$

after a small $\mathbf{k}$ approximation. It is now possible to further assume

$$\tilde{D}_{\mu\nu}(\mathbf{k}) \mapsto k^2 A_{\mu\nu} \tag{1.22}$$

where the important k^2 dependence has been extracted and $A_{\mu\nu}$ is a constant matrix. $U_{\rm tot}$ thus becomes the energy of an ensemble of harmonic oscillators. The equipartition of quadratic degrees of freedom in canonical equilibrium yields

$$\langle \tilde{u}_\mu^*(\mathbf{k})\tilde{u}_\nu(\mathbf{k})\rangle = \frac{k_B T}{k^2}\; A_{\mu\nu}^{-1} \tag{1.23}$$

and a logarithmic divergence of the mean-square displacement

$$\Delta u^2 \equiv \langle |\mathbf{u}(\mathbf{r}) - \mathbf{u}(\mathbf{r}')|^2\rangle \sim k_B T \ln|\mathbf{r}-\mathbf{r}'| \qquad \text{in } \; d = 2 \tag{1.24}$$

follows as a consequence of the logarithmic divergence of the integral $\int d^2k\; k^{-2}$.

An even simpler derivation of the same result goes as follows. Take the harmonic Hamiltonian $H = \frac{c}{2}\int d^d\mathbf{r}\;(\nabla\mathbf{u})^2$ as a starting point. The excitation of a spin-wave with wavelength L (wave vector $2\pi/L$) then requires an energy $E \approx L^d(2\pi/L)^2 \propto L^{d-2}$ that diverges with L for $d = 3$, is independent of L for $d = 2$ (marginal case) and decreases as L^{-1} for $d = 1$.

The divergence of the mean-square displacement in Eqn. (1.24) implies that any atom displaces itself a long distance from each other and hence no long-range order is possible in $d = 2$. This weird effect is due to the dimensionality of space. In three dimensions, the mean square fluctuation is finite.

A more general proof of the lack of positional order in $d \leq 2$ that goes beyond the harmonic approximation was by Mermin (1968). In this paper, he first proposed the following criterion for crystallinity:

$$\begin{aligned} &\tilde{\rho}(\mathbf{k}) = 0 \qquad \text{for } \; \mathbf{k} \; \text{ not a reciprocal lattice vector} \;, \\ &\tilde{\rho}(\mathbf{k}) \neq 0 \qquad \text{for at least one non-zero reciprocal lattice vector} \;, \end{aligned} \tag{1.25}$$

with $\tilde{\rho}(\mathbf{k})$ the Fourier transform of $\rho(\mathbf{r})$, in the thermodynamic limit, that is

$$\tilde{\rho}(\mathbf{k}) = \frac{1}{N}\sum_{i=1}^{N} e^{i\mathbf{k}\cdot\mathbf{r}_i} \;. \tag{1.26}$$

Using Bogolyubov's identity, Mermin showed that the condition (1.25) cannot be satisfied in $d \leq 2$ since in thermal equilibrium at non-vanishing temperature, for all $\mathbf{k}$, $\langle\tilde{\rho}(\mathbf{k})\rangle$ is bounded from above by a quantity that vanishes in the thermodynamic limit.

The possibility of a two-dimensional system with constant density (all Fourier modes vanish) being, however, anisotropic over long distances was left open by Peierls and Landau. The actual definition of the orientational order was also given by Mermin in his 1968 paper. Within the harmonic solid model he simply noticed that

$$\langle[\mathbf{r}(\mathbf{R}+\mathbf{a}_1)-\mathbf{r}(\mathbf{R})]\cdot[\mathbf{r}(\mathbf{R}'+\mathbf{a}_1)-\mathbf{r}(\mathbf{R}')]\rangle \tag{1.27}$$

approaches a_1^2 at long distances $|\mathbf{R}-\mathbf{R}'|\to\infty$, implying that the orientation of the local order is maintained all along the sample. The status of the studies of orientational order in two dimensional systems in the 90s is summarised in (Strandburg, 1992).

Melting scenarii. In $d \geq 3$ melting is a first order phase transition between crystal and liquid (although the details of how this transition occurs are still not fully understood and may depend on the material). In $d = 2$, instead, there is no full consensus yet as to which are the mechanisms for melting and how the passage from solid (with quasi-long-range positional and long-range orientational order) to liquid (with both short-range positional and orientational order) occurs. In the late 70s Halperin & Nelson (1979) and Young (1979) suggested that the transition can occur in two steps, with an intermediate anisotropic *hexatic* phase with short-range positional and quasi-long-range orientational order. Both transitions, between solid and hexatic on the one hand, and hexatic and liquid on the other, were proposed to be driven by the dissociation of topological defects, and therefore be of BKT type:

- In the first stage, at the melting transition T_m, dislocation pairs unbind to form a bond orientationally ordered hexatic liquid.
- In the second stage, at T_i, the disclination pairs which make up the dislocations unbind to form an isotropic liquid.

(These features are sketched in the upper panels in Fig. 1.4.) Moreover, within the KTHNY theory, the *finite size scaling* of the order parameters is expected to be as follows. In the solid phase the translational order parameter should decay with system size as $N^{-\eta}$ with $\eta \leq 1/3$. In the hexatic phase the hexatic order parameter should decay with system size as $N^{-\eta_6}$ with $\eta_6 \to 0$ at the transition with the solid and, according to Nelson & Halperin, $\eta_6 \to 1/4$ at the transition with the liquid. All these conclusions were derived from an RG analysis of the continuous elastic model of a solid separated into the contribution of the smooth displacements and the one of the defects.

A large number of numerical and experimental attempts to confirm (or not) this picture followed. A summary of the situation at the beginning of the 90s can be found in Strandburg (1989, 1992) and close to ten years ago in Gasser (2009). Early numerics and experiments faced some difficulty in establishing the existence of the hexatic phase, and suggested instead coexistence between solid and liquid as expected in a single first order phase transition scenario. However, by the turn of the century the existence of the hexatic phase was settled and quite widely accepted (see the references by Maret

et al. cited below) although evidence for both transitions being of BKT kind remained still elusive.

More recently, Krauth and collaborators (Bernard and Krauth 2011; Engel et al. 2013; Kapfer and Krauth 2015) came back to this problem with powerful numerical techniques and they suggested that, for sufficiently hard repulsive interactions between disks, the transition between the hexatic and liquid phases is of first order. A phenomenon similar to the one put forward by Domany, Schick and Swendsen (1984) with a numerical study, and later shown rigorously by van Enter and Shlosman (2002), would then be at work. Namely, that the BKT transition derived with renormalisation group techniques would be preempted by a first order one. This new scenario allows for co-existence of the liquid and hexatic phases in a finite region of the phase diagram. The mechanisms for the transitions would then be the following.

- In the first stage, at T_m, dislocation pairs unbind to form a bond orientationally ordered hexatic phase.
- In the second stage, at T_i, grain boundaries made of strings of alternating five and seven fold defects would percolate across the sample and liquify it.

While real time video microscopy on superparamagnetic colloids interacting via a *soft* r^{-3} *potential* tend to confirm the KTHNY scenario (Zahn, Lenke and Maret, 1999; Zahn and Maret, 2000; Von Grünberg, Keim and Maret, 2007; Keim, Maret and Von Grünberg, 2007; Gasser, Eisenmann, Maret and Keim, 2010), experimental evidence for the new scenario in a colloidal *hard disks* system was recently given by Thorneywork *et al.* (2017). It seems plausible that the mechanism for melting in $2d$ be non-universal and depend on the interaction potential and other specificities of the systems. Indeed, the numerical simulations prove that for sufficiently soft potential the first order transition is replaced by the conventional BKT one (Kapfer and Krauth, 2015). Moreover, a choice between the two is also made by the *form* of the particles: the polygon case was carefully studied by Anderson *et al.* (2017) and a dependence of the order of the transition with the number of sides of the constituent polygons was claimed in this paper.

1.4.2 Effects of interactions on dilute systems: the equation of state

Since we may be dealing with first order phase transitions, it is useful to recall how these arise in the best known case of the liquid-gas transition and how they lead to co-existence. This is seen, for instance, from the equation of state derived under various approximations. For example, the virial expansion is a common technique used to study weakly interacting gases with perturbative methods. It is explained in many textbook, see *e.g.* (Kardar, 2007), and we will not reproduce much details here. In short, the virial expansion expresses the deviations from the ideal gas equation of state, $PV = Nk_BT = nRT$ with $n = N/N_A$ the number of atoms over Avogadro's number and $R = k_BN_A$ the gas constant, as a power series in the density $\rho = N/V$ with temperature dependent coefficients. Truncated to order ρ^2, this expansion yields the *Van der Waals equation* $P_{\text{eff}}V_{\text{eff}} = (P + aN^2/V^2)(V - bN) = nRT$ (where the effective volume takes into account the reduction due to the space occupied by the particles themselves and the effective pressure is higher than the bare one due to the attraction between the particles). The latter breaks the positivity requirement

on the isothermal compressibility $\kappa_T = -V^{-1}\partial V/\partial P|_T$ that is a consequence of its fluctuation-dissipation relation (in the grand canonical ensemble) with the variance of the particle number confined to the volume V,

$$\kappa_T = \frac{1}{k_B T}\frac{V}{\langle N\rangle^2}\langle(N-\langle N\rangle)^2\rangle \geq 0\,. \tag{1.28}$$

In physical terms, a system with negative compressibility is unstable and it would collapse. Indeed, the Van der Waals isotherms have a portion with negative compressibility that indicates an instability towards formation of domains of low and high density, in other words, phase separation between liquid and gas, both with positive compressibility. For volumes in this region, the isotherms of the real system are instead flat due to the coexistence of the two phases (see Fig. 1.6 (a)). The *Maxwell construction*, an equilibrium argument, indicates that the stability of the sample is obtained at a value of the pressure P (that determines the volumes occupied by the two phases) such that the areas above and below the dip and peak of the $P(V)$ curve are the same.

In a real system with finite size, the isotherms also show a Mayer-Wood loop structure (Mayer and Wood, 1965). However, one has to be careful before concluding that such a loop is due to a first order phase transition. Actually, finite systems undergoing a second order transition may also show one (Alonso and Fernández, 1999). The scaling of the loop area with system size does, instead, provide unambiguous evidence for first order phase transitions. Indeed, if there is a coexistence region, the system should hold in it an interface between the two macroscopic phases. The surface occupied by this interface should scale as L^{d-1} (ignoring possible fractal phenomena) and the free-energy cost of it should therefore be $\Delta F \propto L^{d-1}$ leading to a free-energy density cost of $\Delta f \propto L^{d-1}/L^d = L^{-1}$ that, in $d = 2$ corresponds to $N^{-1/2}$. The free-energy density can be derived from the equation of state *via* an integration since $P = -\partial F/\partial V|_T$ that implies that the area occupied by the loop should decrease with system size as $N^{-1/2}$.

1.5 Active systems

We now enter the field of active systems. We very briefly mention in this Section the results of numerical studies that led us to construct the phase diagrams [in the (Pe, ϕ) plane] of the active Brownian particle and active dumbbell systems. When constructing these phase diagrams we seriously took into account the knowledge of the passive limit behaviour that we have described so far.

1.5.1 Numerical methods

We will not expose here the numerical methods used to integrate the dynamics of passive and active matter system as there exist excellent textbooks and review articles in the literature that explain in detail these techniques (Allen and Tildesley, 1989). In a few words, the integration of Eqns (1.1) is typically done with the velocity Verlet algorithm (Rahman, 1964; Verlet, 1967) that can be easily parallelised, and this is done using the LAMMPS method (Plimpton, 1995).

It is important to note, though, that while in equilibrium statistical averages are usually exchanged with time averages under the *ergodic hypothesis*, out of equilibrium this hypothesis cannot be taken for granted and statistical averages may need to be done by definition, that is, by averaging over many samples run under the same conditions.

Numerical simulations suffer from severe limitations given by the typically small size of the systems compared to the thermodynamic limit in which theoretical calculations are performed. Furthermore, the dynamic equations are integrated over relatively short times. In the context of active matter, these two limitations can, however, represent the actual experimental situation as real systems do not count with constituents as numerous as the Avogadro number and time-scales can be relatively short as well. In finite size systems, special care has to be taken with the choice of boundary conditions and how these may affect the behaviour of the system in the bulk. Periodic boundary conditions are often chosen since they tend to minimise finite-size effects, not having edges, but they also avoid the annoying decision to make concerning interactions between particles and walls. Special care has to be taken not to inhibit periodic or orientational order or symmetry with this choice.

Having said this, we are interested in determining phase diagrams that exist in the thermodynamic limit. Finite size scaling should therefore be used to determine the behaviour in the infinite size limit. Typical simulations ran with $N = 256^2$ particles, scanning the parameter space $\phi \in [0 : 0.9]$ and $\mathrm{Pe} \in [0 : 200]$. Notice that since the disks are not completely hard, some overlap between them is possible and values of ϕ that are slightly larger than the close packing limit can be accessed in the simulation (recall that the close packing fraction of disks in two dimensions is achieved by a perfect triangular lattice and it amounts to $\phi_{\mathrm{cp}} \approx 0.91$).

1.5.2 Phase diagrams

Passive systems in two dimensions have liquid (short range order for both translation and bond orientation order), hexatic (short range order translation and quasi long range order for bond orientation order) and solid (quasi long range order for translation and long range for bond orientation order) phases. The fact that there is co-existence between liquid and hexatically ordered phases in systems of passive, purely repulsive, disks was evidenced by Bernard, Kampfer & Krauth, in a series of papers, if the potential is hard enough. The question naturally arises as to whether the passive phases, and the co-existence region, survive under activity, and whether they do both for spherically symmetric and asymmetric elements.

The various phases can be examined with the usual observables already defined and mentioned in the context of the passive limit: order parameters, their correlation functions, the distributions of their local values, their fluctuations, and the pressure loop (if accepted, see below).

We will not include here all the evidence for these claims, that can be found in the relevant references, and give rise to the two phase diagrams in the (Pe, ϕ) plane shown in Fig. 1.5 (a) for the active disks and (b) for the active dumbbells. The colour code is such that white is liquid (or gas), grey is coexistence, blue is hexatic, and yellow is solid (in Sec. 1.5.4 we will explain why we have not distinguished hexatic from solid

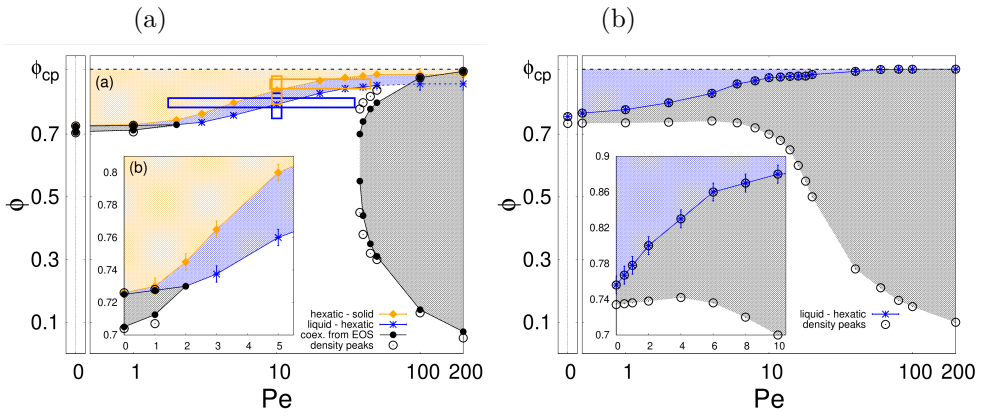

Fig. 1.5 The phase diagrams of interacting active Brownian disks (a) and dumbbells (b) as obtained by Digregorio *et al.* (2018) for the disks [see also Klamser *et al.* (2018)] and Cugliandolo *et al.* (2017) and Petrelli *et al.* (2018) for the dumbbells. The insets are zooms over the small Pe regions, close to $\phi = 0.7$. The colour code is such that in the grey regions there is coexistence, while the system exhibits hexatic order and is in the solid phase in the purple and orange regions, respectively.

in the dumbbell system and why we have depicted all the region above the end of coexistence in blue). We will simply discuss in the following paragraphs some aspects of the structure of these systems.

In both cases there is a region with co-existence (grey) that penetrates the phase diagram along the Pe $\gtrsim 0$ direction, close to $\phi \simeq 0.7$. The dilute phase has no order and behaves as an active liquid or gas while the dense phase next to it has orientational order and it is therefore an active hexatic phase. However, we see a difference. While for disks this coexistence ends at a relatively small value of Pe and the so-called *motility induced phase separation* (MIPS) region appears for much larger values of Pe, for dumbbells the region with coexistence simply merges (or is the same as) what is usually called MIPS. We will not discuss here the transition between the active hexatic (blue) and the active solid (yellow) phases.

1.5.3 The equation of state

The mere definition of pressure needs attention in active matter systems. In mechanical terms, it is the force per unit surface exerted by the system on the walls of its container. In equilibrium in the thermodynamic limit, the mechanical pressure is also given by an *equation of state* that relates it to bulk properties of the system, namely, temperature and density, with no reference of the particular interaction potential between constituents and boundary walls. This relation is not at all obvious out of equilibrium, and it has been observed in some active matter systems that the pressure does depend on the interaction potential details. This issue will be covered in other Chapters in this book.

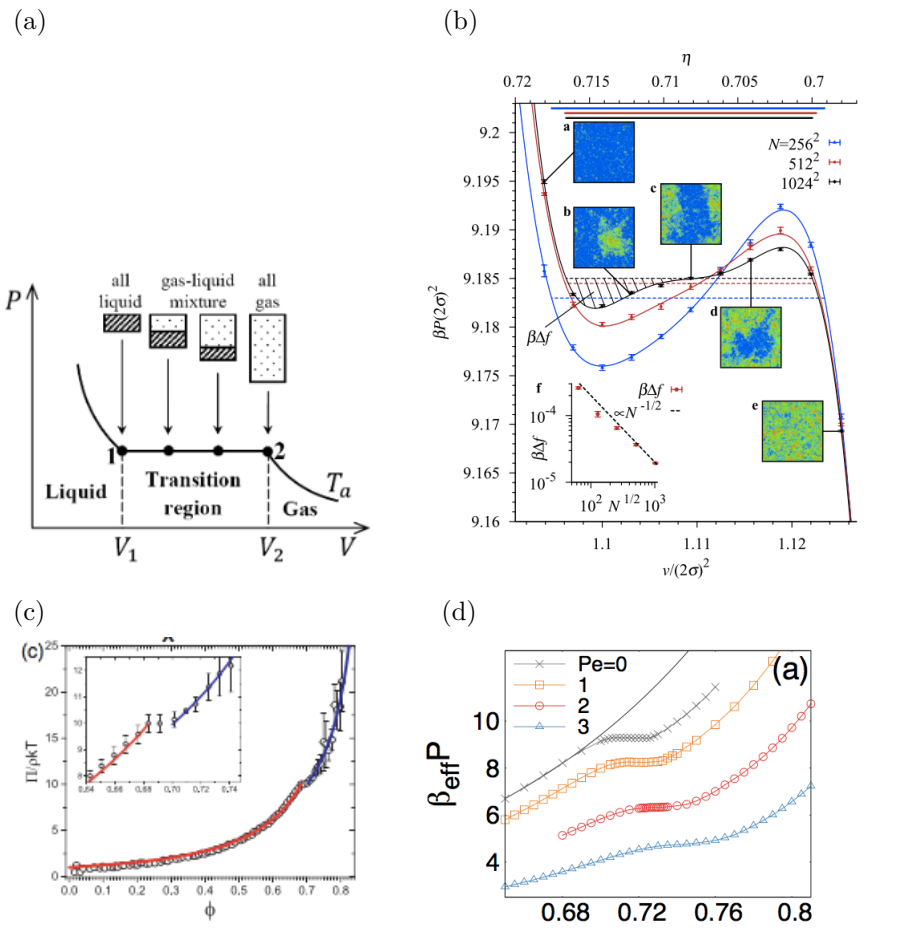

Fig. 1.6 The equation of state. (a) The van der Waals equation. (b) Simulation of hard disks from Bernard & Krauth (2011). (c) Experiments on hard disks from Thorneywork *et al.* (2017). (d) Simulations of active hard disks from Digregorio *et al.* (2018).

Expressions for the mechanical pressure for spherically symmetric constituents governed by a *Markov stochastic process of Langevin kind* both under and over damped for confined and periodic boundary conditions, were recently derived. Moreover, formulæ for ensembles of active Brownian particles in interaction (Winkler, Wysocki and Gompper, 2015) and active dumbbells also in interaction (Joyeux and Bertin, 2016) were also recently deduced and discussed. In cases in which the constituents are not symmetric there is some ambiguity related to the way in which the interactions with the walls should be considered; we will not discuss this issue further here.

Figure 1.6 displays four panels with the equation of state of (a) the van der Waals equation, (b) the numerical simulations of a rather hard disk passive system from Bernard & Krauth (2011), (c) the experimental measurements of another rather hard

disk passive ensemble from Thorneywork *et al.* (2017), and (d) the numerical simulations of an ensemble of active Brownian disks at small Pe from Digregorio *et al.* (2018). All plots are quite similar and were used to claim that the transition is of first order in the (b), (c) and (d) cases. In the case of active Brownian particles, these measurements were used to locate datapoints that yield the boundaries of the co-existence region (and coincide with the location of the boundary estimated from the distribution of local densities and local hexatic order parameter).

1.5.4 Phase separation in the dumbbell system

We will end this presentation giving some details on the phase separation found in the dumbbell system, with molecules made of two joined disks with the same disk diameter σ_d and distance between their centres very close to $2\sigma_d$ and almost constant over time. A much more exhaustive discussion of the structure and dynamics of this model can be found in (Petrelli *et al.*, 2018).

Take the passive dumbbell system at a given global density with co-existence. As the activity is turned on, some spatial regions get denser, leaving away disordered holes. Under increasing activity, the high density peak in the bimodal distribution of local densities continuously moves towards higher values and its weight increases while the low density peak moves in the opposite direction and its weight decreases. As far as density is concerned we do not see any discontinuity when moving towards higher activities in the coexistence region. A similar behaviour is observed when following the local hexatic order parameter. Curves of constant repartition of dense and loose phases can be traced and the system's behaviour can be compared on these. This is different in the active Brownian disk system, for which the region with coexistence at low Pe ends on curves at relatively low values of Pe, see the phase diagrams shown in Fig. 1.5.

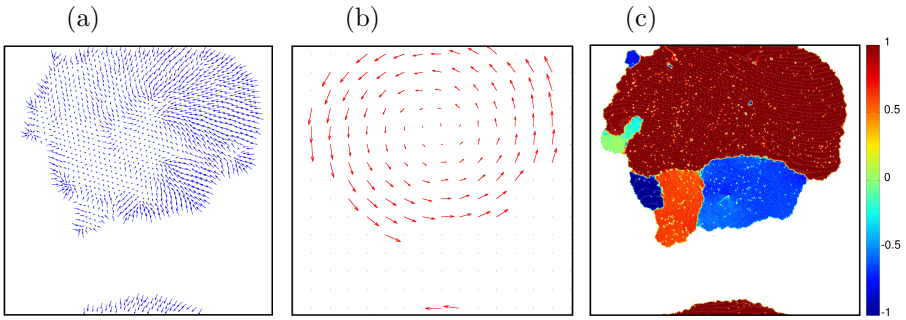

Fig. 1.7 Dumbbells at a global packing fraction such that the system is in the coexistence region with 50-50 proportion of liquid and hexatic phases, Pe = 200. Panel (a) shows the dumbbells polarisation, panel (b) the local velocity and (c) the local hexatic order parameter. The figure is taken from Petrelli *et al.* (2018).

Depending on the strength of the activity, this dynamic process allows the dumbbells in the ordered regions to pack in a single domain with perfect hexatic order, or

in polycrystalline arrangements concerning the orientational order, see panel (c) in Fig. 1.7.

Another interesting observable to characterise the structure and dynamics of the clusters is the coarse-grained *polarisation* or, basically, a vector constructed as the average over a coarse-graining volume of the sum of vectors pointing from head-to-tail on each dumbbell, see panel (a) in Fig. 1.7. At $\mathrm{Pe} = 0$ there is no polar order whatsoever (not even locally). At intermediate activity, say $\mathrm{Pe} = 40$, the clusters show an aster polar configuration with a defect at the centre (basically on the dumbbell that triggered aggregation and the subsequent formation of the cluster). At larger activity, say $\mathrm{Pe} = 200$, the aster evolves to a spiralling pattern (see the map in the figure) and the cluster consequently rotates, a motion that is not observed at lower Pe, see Fig. 1.7. We therefore found that polar order differentiates between clusters at small and high activity.

Interest can then be set on the motion of the dumbbells. In the phase separated cases, the dumbbells in the dilute phase are basically free, since their *kinetic energy* is very close to the one of independent dumbbells for all Pe values. The kinetic energy of the dumbbells in the dense phase, instead, increases very weakly with activity, due to the fact that the mobility is suppressed inside the clusters and these are massive and move very slowly.

While the kinetic energy gives a measure of the strength of flow in the system, the *enstrophy* is a measure of the presence of vortices in the velocity field and it can be used to understand whether clusters rotate driven by activity. For high values of the activity the dumbbells arrange in spirals, the clusters in the system undertake a rotational motion and the probability distribution function of the enstrophy develops a multi-peak structure associated to the rotating clusters. A comparison between the velocity and the polarisation fields shows that the former exhibits a vortex pattern while the polarisation one is a spiral.

For strong enough Pe, say $\mathrm{Pe} > 50$, the spontaneously formed clusters turn around their centre of mass with an angular velocity that is proportional to the inverse of their radii. The poly-crystalline nature of the clusters, with respect to the hexatic order, does not seem to play a major role in their rotational properties. Instead, the orientation of the dumbbells inside the clusters is, indeed, important, as a certain amount of disorder in the form of misalignment is needed to make them turn.

The exact nature of the transition between the hexatic and solid phases for the dumbbell system and its location in the phase diagram are still open questions. Since monomers are constrained to be attached in pairs, they cannot arrange on a triangular lattice at any $\phi < \phi_{\mathrm{cp}}$ forcing the positional correlations of the monomers to decay exponentially. It is therefore hard to identify the solid phase and this is the reason why in Fig. 1.5 (b) we show all the region of the phase diagram lying above the end of coexistence in blue.

1.6 Concluding remarks

The motivation for the studies of active systems in two dimensions described here was to determine their full phase diagram linking the strong activation limit (usually

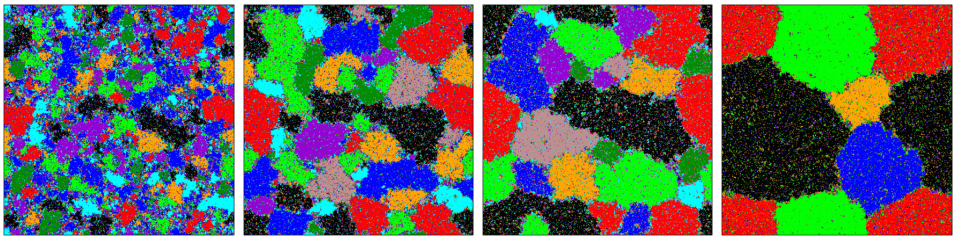

Fig. 1.8 Four snapshots taken at subsequent times that are representative of the dynamics following a quench across the first order transition of the Potts model with $q = 9$. Each colour represents one state among the nine possible ones of the spins. Figure taken from Corberi *et al.* (2018).

studied in the active matter literature) to the passive case (already a very hard and not yet settled problem).

Many open questions remain unanswered and pose important challenges. We comment on a few of them below.

The first issue that calls for a careful analysis is how does the phase diagram transform from the one for disks to the one for dumbbells when one smoothly varies the form of the molecules to interpolate between these two limits.

A careful study of the dynamics of the topological defects and their influence upon the phase transitions is definitely needed. Qi *et al.* (2014) and Kapfer & Krauth (2015) suggested that there is a percolation of the defect string network at the liquid-hexatic transition of passive models with sufficiently hard potentials, and that these strings surround domains with hexatic order. Is it the case for the active model as well?

In equilibrium a duality transformation linking the interacting defect system relevant for two-dimensional melting to a Laplacian roughening model is often used to attack the former by simulating the latter. However, such a relation does not necessarily hold under active forces since it relies on a transformation of the partition function. Are there other transformations of similar kind that could be used in the active case?

The hexatic phase is only stable in a minute density regime in the case of hard disks, which can be missed very easily in both simulations and experiments. Additionally, the order of the transition is difficult to ascertain due to finite-size effects. Therefore, although the picture that we described here is consistent and very attractive, it still needs to be confirmed with more detailed numerically simulations and, hopefully, experimental measurements. A rigorous proof, as the one developed by van Enter and Shlosman (2002) for the planar spin model seems out of reach for the active model since it is specific to equilibrium conditions (Gibbs states, partition functions). Could any other kind of rigorous proof be worked out for the active case?

The dynamics across a first order phase transition occurs *via* nucleation of the stable phase into the unstable one. This problem is usually discussed with a single state that wins the competition against another one when the transition is crossed. A slightly more complex example is the one of the Potts model with $q > 4$, a model in which the stable states in the ordered phase are q degenerate ones, and the relevant dynamic process is a multi-nucleation one. If many stable phases of different

kind nucleate simultaneously these will grow quickly until they touch and block. The further evolution is a normal coarsening one. The time-scales for nucleation, growth of sufficiently large bubbles and coarsening are very different and can be numerically quantified exploiting data from Monte Carlo simulations (Corberi, Cugliandolo, Esposito and Picco, 2018). The dynamics across the first order liquid-hexatic transition should have similar features to the ones just described. This problem is under study in our group.

References

Alder, B. J. and Wainwright, T. E. (1962). Phase transition in elastic disks. Phys. Rev., **127**, 359.

Allen, M. P. and Tildesley, D. J. (1989). Computer simulation of liquids. Oxford University Press.

Alonso, J. and Fernández, J. (1999). Van der waals loops and the melting transition in two dimensions. Phys. Rev. E, **59**, 2659.

Amit, D. J. (1984). Field theory, the renormalization group and critical phenomena. World Scientific, Singapore.

Anderson, J. A., Antonaglia, J., Millan, J. A., Engel, M., and Glotzer, S. C. (2017). Shape and symmetry determine two-dimensional melting transitions of hard regular polygons. Phys. Rev. X, **7**, 021001.

Ashcroft, N. W. and Mermin, N. D. (1976). Solid State Physics. Harcourt College Publisher, Forth Worth. Ch. 22, Classical Theory of the Harmonic Crystal.

Berezinskii, V. L. (1971a). Destruction of long-range order in one-dimensional and two-dimensional systems having a continuous symmetry group i. classical systems. Zh. Eksp. Teor. Fiz., **59**, 907.

Berezinskii, V. L. (1971)b). Destruction of long-range order in one-dimensional and two-dimensional systems having a continuous symmetry group ii. quantum systems. Zh. Eksp. Teor. Fiz., **61**, 1144.

Bernard, E. and Krauth, W. (2011). Two-step melting in two dimensions: First-order liquid-hexatic transition. Phys. Rev. Lett., **107**, 155704.

Blanc, X. and Lewin, M. (2015). The crystallization conjecture: A review. EMS Surveys in Mathematical Sciences, **2**, 255.

Bogoliubov, N. N. (1962). Phys. Abhandl. S. U., **6**, 113.

Cardy, J. (1996). Scaling and renormalization in Statistical Physics. Cambridge University Press, Cambridge.

Comaron, P., Dagvadorj, G., Zamora, A., Carusotto, I., Proukakis, N. P., and Szymańska, M. H. (2018). Dynamical critical exponents in driven-dissipative quantum systems. Phys. Rev. Lett., **121**, 095302.

Corberi, F., Cugliandolo, L. F., Esposito, M., and Picco, M. (2018). Multi-nucleation in the first-order phase transition of the 2d potts model.

Cugliandolo, L. F. (2011). The effective temperature. J. Phys. A, **44**, 483001.

Cugliandolo, L. F., Digregorio, P., Gonnella, G., and Suma, A. (2017). Phase co-existence in bidimensional passive and active dumbbell systems. Phys. Rev. Lett., **119**, 268002.

Digregorio, P., Levis, D., Cugliandolo, L. F., Gonnella, G., Pagonabarraga, I., and Suma, A. (2018). Full phase diagram of active brownian disks: from melting to motility-induced phase separation. Phys. Rev. Lett., **212**, 098003.

Domany, E., Schick, M., and Swendsen (1984). First-order transition in an XY model with nearest-neighbor interactions. Phys. Rev. Lett., **52**, 1535.

Engel, M., Anderson, J. A., Glotzer, S. C., Isobe, M., Bernard, E. P., and Krauth, W. (2013). Hard-disk equation of state: First-order liquid-hexatic transition in two dimensions with three simulation methods. Phys. Rev. E, **87**, 042134.

Fily, Y., Henkes, S., and Marchetti, M. C. (2014). Freezing and phase separation of self-propelled disks. Soft Matter, **10**, 2132.

Fily, Y. and Marchetti, M. C. (2012). Athermal phase separation of self-propelled particles with no alignment. Phys. Rev. Lett., **108**, 235702.

Gasser, U. (2009). Crystallization in three- and two-dimensional colloidal suspensions. J. Phys.: Cond. Matt., **21**, 203101.

Gasser, U., Eisenmann, C., Maret, G., and Keim, P. (2010). Melting of crystals in two dimensions. ChemPhysChem, **11**, 963.

Goldenfeld, N. (1992). Lectures on phase transitions and the renormalization group. Addison-Wesley, Reading.

Henkes, S., Fily, Y., and Marchetti, M. C. (2011). Active jamming: self-propelled soft particles at high density. Phys. Rev. E, **84**, 040301 (R).

Herbut, I. (2006). A modern approach to critical phenomena. Cambridge University Press, Cambridge.

Jelić, A. and Cugliandolo, L. F. (2011). Quench dynamics of the 2*d* XY model. J. Stat. Mech. Theory Exp., P02032.

Jonsson, A., Minnhagen, P., and Nylen, M. (1993). New critical-point for 2-dimensional XY-type models. Phys. Rev. Lett., **70**, 1327.

Joyeux, M. and Bertin, E. (2016). Pressure of a gas of underdamped active dumbbells. Phys. Rev. E, **93**, 032605.

Kapfer, S. and Krauth, W. (2015). Two-dimensional melting: From liquid-hexatic coexistence to continuous transitions. Phys. Rev. Lett., **114**, 035702.

Kardar, M. (2007). Statistical Physics of Particles. Cambridge University Press, Cambridge.

Keim, P., Maret, G., and Von Grünberg, H. H. (2007). Frank's constant in the hexatic phase. Phys. Rev. E, **75**, 031402.

Klamser, J. U., Kapfer, S. C., and Krauth, W. (2018). Thermodynamic phases in two-dimensional active matter. nat. Comm., **9**, 5045.

Kosterlitz, J. M. (1974). Critical properties of 2-dimensional XY model. J. Phys. C-Solid State Physics, **7**, 1046.

Kosterlitz, J. M. (2016). Kosterlitz-Thouless physics: a review of key issues. Reports Prog. Phys., **79**, 026001.

Kosterlitz, J. M. and Thouless, D. J. (1972). Long range order and metastability in two dimensional solids and superfluids. (application of dislocation theory). J. Phys. C-Solid State Physics, **5**, L124.

Kosterlitz, J. M. and Thouless, D. J. (1973). Ordering, metastability and phase transitions in two-dimensional systems. J. Phys. C-Solid State Physics, **6**, 1181.

Landau, L. D. (1937a). On the theory of phase transitions i. Phys. Z. Sowjet, **11**, 26.

Landau, L. D. (1937b). On the theory of phase transitions ii. Phys. Z. Sowjet, **11**, 545.

Levis, D. and Berthier, L. (2014). Clustering and heterogeneous dynamics in a kinetic monte carlo model of self-propelled hard disks. Phys. Rev. E, **89**, 062301.

Loi, D., Mossa, S., and Cugliandolo, L. F. (2011). Effective temperature of active complex matter. Soft Matter, **7**, 3726–3729.

Mayer, J. E. and Wood, W. W. (1965). Interfacial tension effects in finite, periodic, two dimensional systems. J. Chem. Phys., **42**, 4268.

Mermin, N. D. (1968). Crystalline order in two dimensions. Phys. Rev., **176**, 250.

Mie, G. (1903). Zur kinetischen theorie der einatomigen körper. Annalen der Physik, **11**, 657.

Minnhagen, P. (1987). The two-dimensional coulomb gas, vortex unbinding, and superfluid-conducting films. Rev. Mod. Phys., **59**, 1001.

Nelson, D. R. and Halperin, B. I. (1979). Dislocation-mediated melting in two dimensions. Phys. Rev. B, **19**, 2457.

Parisi, G. (1988). Statistical field theory. Addison-Wesley, Reading.

Peierls, R. E. (1934). Bemerkungen über umwandlungstemperaturen. Helv. Phys. Acta Supp. II, **7**, 91.

Petrelli, I., Digregorio, P., Cugliandolo, L. F., Gonnella, G., and Suma, A. (2018). Active dumbbells: dynamics and morphology in the coexisting region. Eur. Phys. J. E, **41**, 128.

Plimpton, S. (1995). Fast parallel algorithms for short-range molecular dynamics. J. Comp. Phys., **117**, 1.

Qi, W., Gantapara, A. P., and Dijkstra, M. (2014). Two-stage melting induced by dislocations and grain boundaries in monolayers of hard spheres. Soft Matter, **10**, 5449.

Rahman, A. (1964). Correlations in the motion of atoms in liquid argon. Phys. Rev., **136**, A405.

Redner, G. S., Hagan, M. F., and Baskaran, A. (2013). Structure and dynamics of a phase-separating active colloidal fluid. Phys. Rev. Lett., **110**, 055701.

Redner, G. S., Wagner, C. G., Baskaran, A., and Hagan, M. F. (2016). Classical nucleation theory description of active colloid assembly. Phys. Rev. Lett., **117**, 148002.

Simon, B. (1997). Phase Transitions and Collective Phenomena. Cambridge University Press, Cambridge.

Stanley, H. E. (1971). Introduction to phase transitions and critical phenomena|. Oxford University Press, New York.

Strandburg, K. J. (ed.) (1992). Bond-Orientational Order in Condensed Matter Systems, Heidelberg. Springer-Verlag.

Thorneywork, A. L., Abbott, J. L., Aarts, D. G. A. L., and Dullens, R. P. A. (2017). Two-dimensional melting of colloidal hard spheres. Phys. Rev. Lett., **118**, 158001.

Van Enter, A. C. D. and Shlosman, S. B. (2002). First-order transitions for n-vector models in two and more dimensions: Rigorous proof. Phys. Rev. Lett., **89**, 285702.

Verlet, L. (1967). Computer "experiments" on classical fluids. i. thermodynamical properties of lennard-jones molecules. Phys. Rev., **159**, 98.

Von Grünberg, H. H., Keim, P., and Maret, G. (2007). Phase transitions in two-dimensional colloidal systems. In Colloidal order: entropic and surface forces (ed.

G. Gompper), p. 40. Wiley, Weinheim.
Weeks, J. D., Chandler, D., and Andersen, H. C. (1971). Role of repulsive forces in determining the equilibrium structure of simple liquids. J. Chem. Phys., **54**, 5237.
Winkler, R. G., Wysocki, A., and Gompper, G. (2015). Virial pressure in systems of spherical active brownian particles. Soft Matter, **11**, 6680.
Young, A. P. (1979). Melting and the vector coulomb gas in two dimensions. Phys. Rev. B, **19**, 1855.
Zahn, K., Lenke, R., and Maret, G. (1999). Two-stage melting of paramagnetic colloidal crystals in two dimensions. Phys. Rev. Lett., **82**, 2721.
Zahn, K. and Maret, G. (2000). Dynamic criteria for melting in two dimensions. Phys. Rev. Lett., **85**, 3656.
Zukovic, M. and Kalagov, G. (2017). XY model with higher-order exchange. Phys. Rev. E, **96**, 022158.